

Supporting Information

Observation of Piezoelectricity in Lead-free $\text{Cs}_2\text{AgBiBr}_6$ Perovskite: A New Entrant in Energy Harvesting Arena

Tufan Paul^{1#}, Aditi Sahoo^{2#}, Soumen Maiti³, Suvankar Mandal⁴, Souvik Bhattacharjee⁴,
Avishek Maiti⁵, Kalyan Kumar Chattopadhyay*^{1,4}

¹*School of Material Science and Nanotechnology, Jadavpur University, Kolkata-700032, India*

²*CSIR- Central Glass and Ceramic Research Institute, Kolkata-700032, India*

³*St Thomas College of Engineering & Technology, Kolkata, 700023, India*

⁴*Department of Physics, Jadavpur University, Kolkata, 700032, India*

⁵ *S. N. Bose National Centre for Basic Sciences, Salt Lake, Kolkata 700106, India*

*Corresponding author Email: kalyan_chattopadhyay@yahoo.com

Current affiliation: Institut national de la recherche scientifique (INRS), EMT Centre, Varennes, Quebec J3X 1S2, Canada

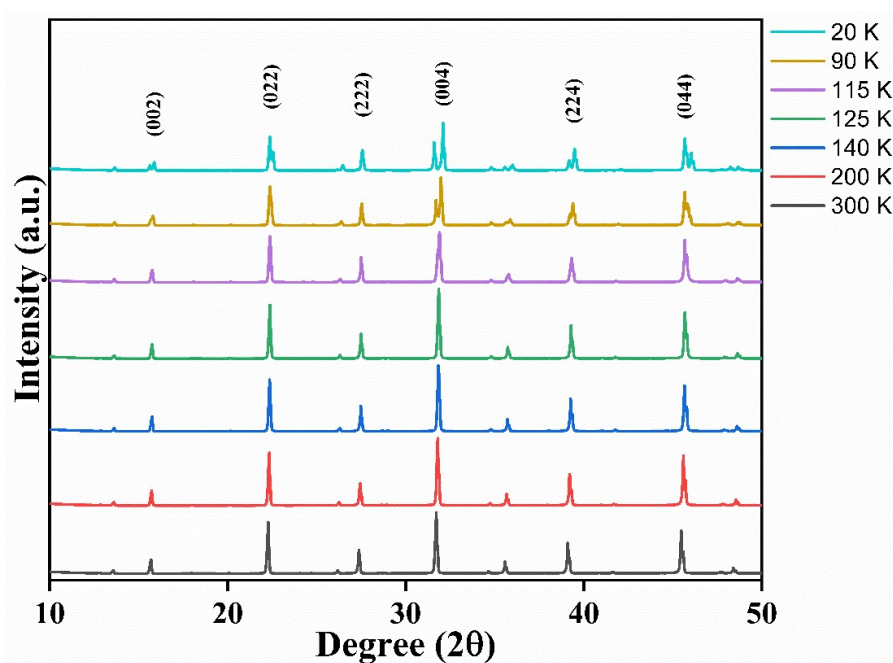


Figure S1: Low temperature dependent XRD of $\text{Cs}_2\text{AgBiBr}_6$.

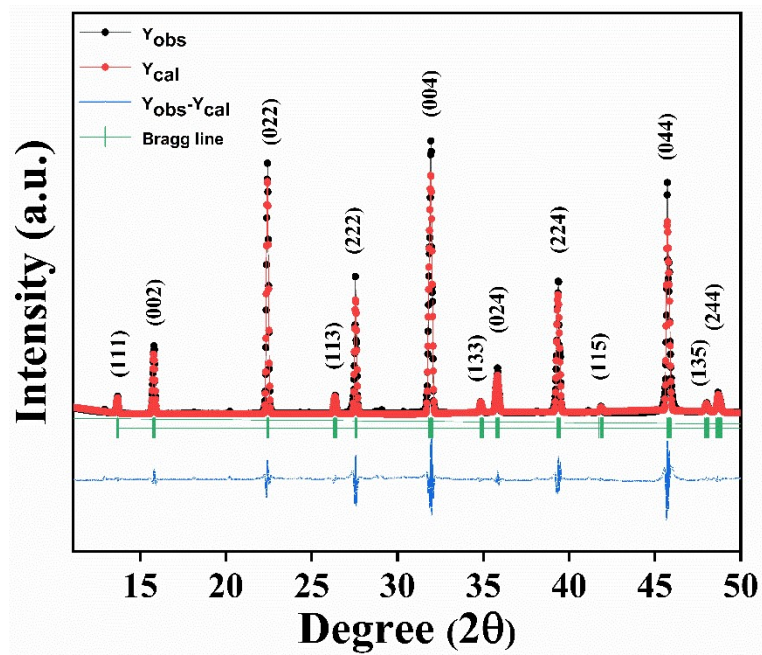


Figure S2: Refined XRD data of $\text{Cs}_2\text{AgBiBr}_6$ at 115 K in tetragonal lattice system with $I4/m$ space group.

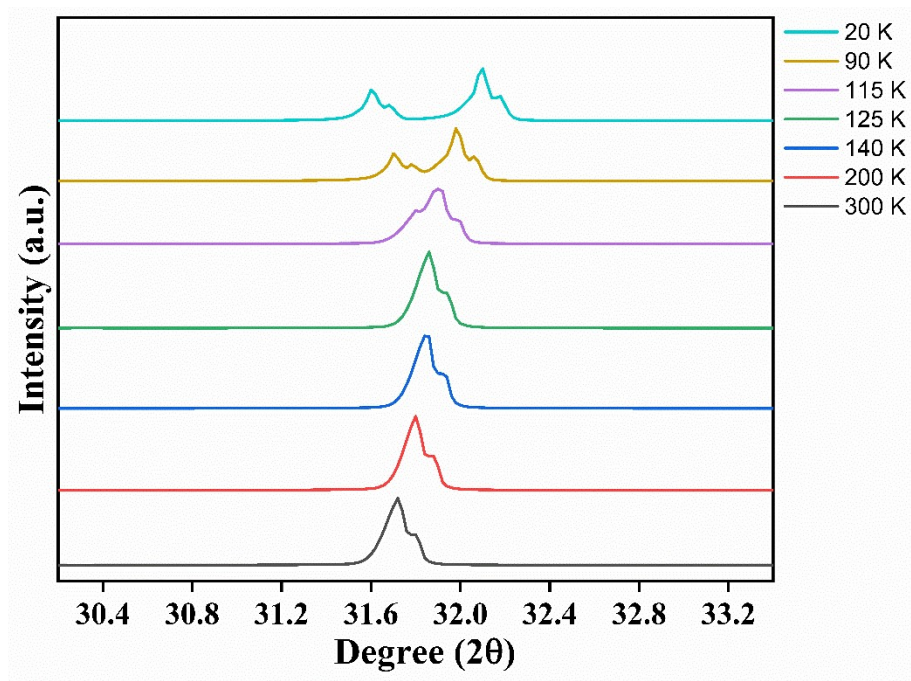


Figure S3: Low temperature XRD of $\text{Cs}_2\text{AgBiBr}_6$ at the phase transition region.

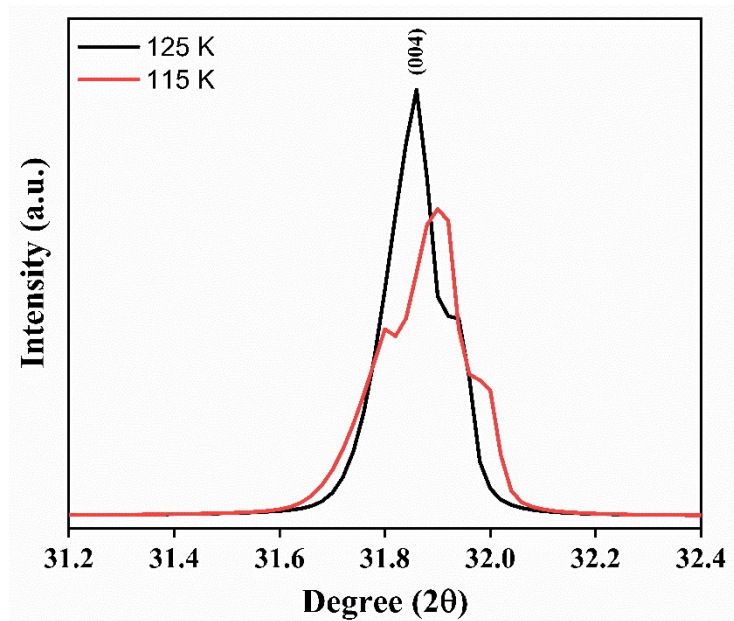


Figure S4: Zoom view of 31.73° peak at low temperature XRD of $\text{Cs}_2\text{AgBiBr}_6$.

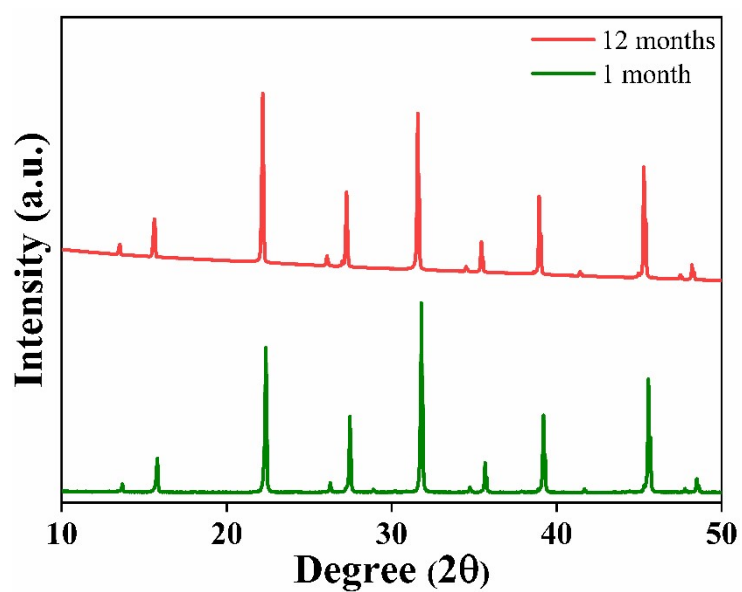


Figure S5: Time dependent XRD stability of $\text{Cs}_2\text{AgBiBr}_6$.

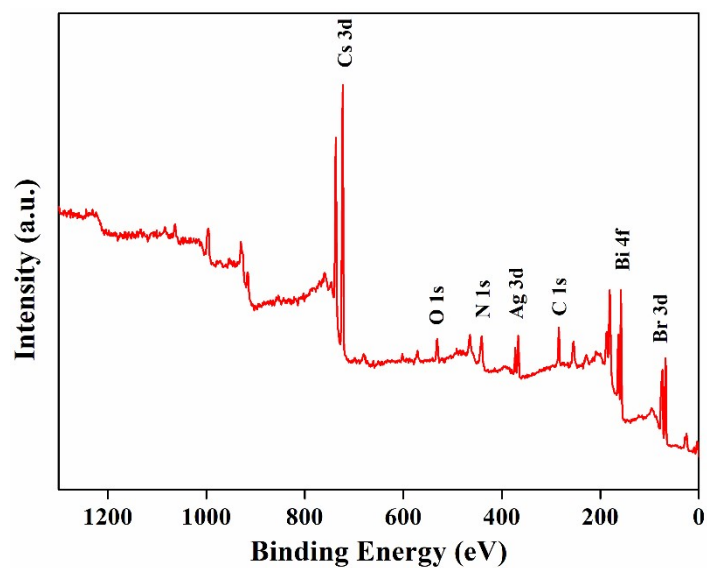


Figure S6: XPS survey scan of $\text{Cs}_2\text{AgBiBr}_6$.

Table S1: Comparison of Piezoresponse of various halide perovskites

S. No.	Material	Maximum piezoelectric Amplitude response	Applied electric bias	Reference
1.	FASnI_3	~400 pm	± 10 V	1
2.	$\gamma\text{-CsPbI}_3$	~350 pm	± 10 V	2
3.	CsGeBr_3	~70 pm	± 8 V	3
4.	$\text{PEA}_2\text{MA}_{n-1}\text{Pb}_n\text{I}_{3n+1}$ (n =5)	~400 pm	± 10 V	4
5.	$\text{MAPb}(\text{I}_{1-x}\text{Br}_x)_3$	~90 pm	± 5 V	5
6.	DMAACdCl_3	~175 pm	± 60 V	6
7.	$(\text{TMAEA})\text{Pb}_2\text{Cl}_6$	~600 pm	± 20 V	7
8.	$\text{Cs}_2\text{AgBiBr}_6$	~272 pm	± 20 V	this work

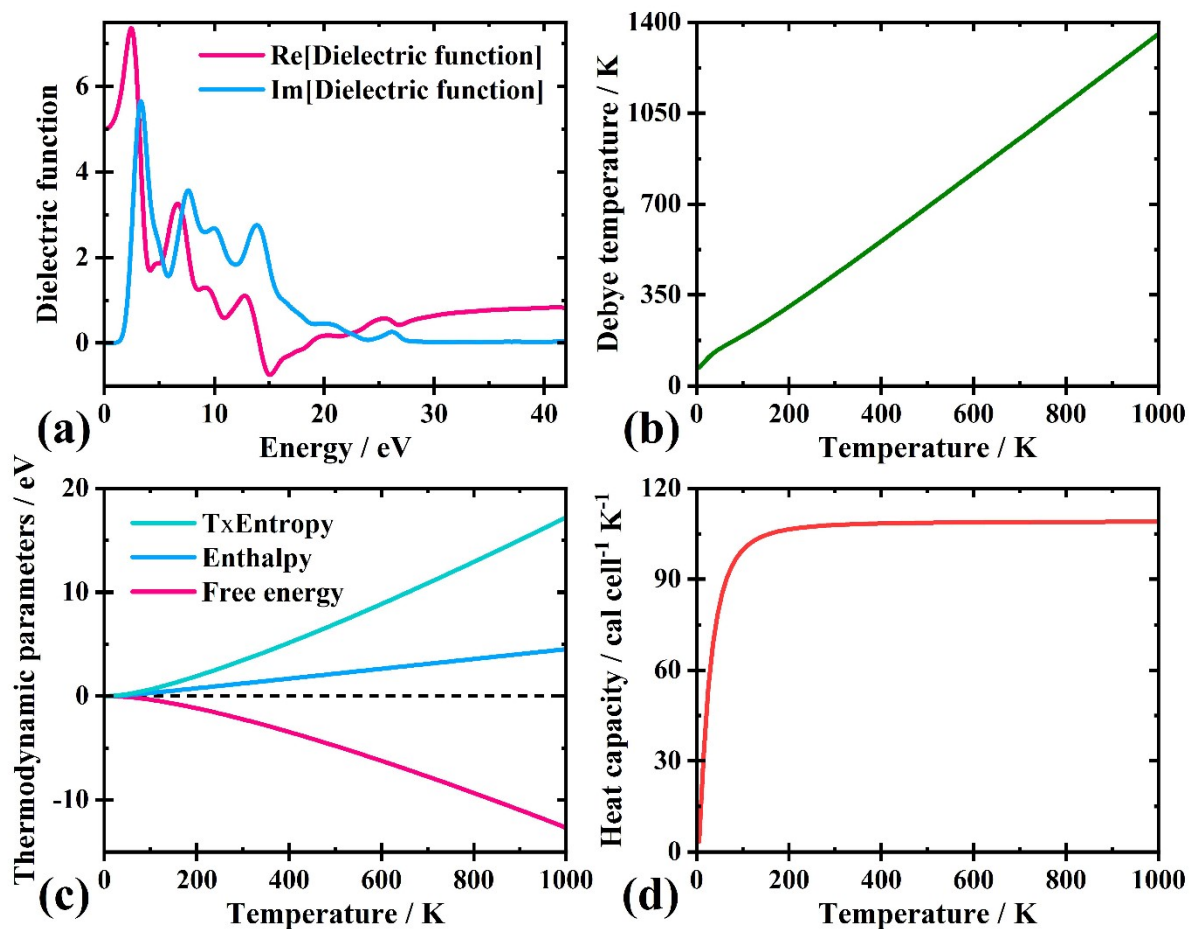


Figure S7: (a) Energy dispersive real and imaginary parts of optical dielectric function; (b) Debye temperature versus absolute temperature (T); (c) $T \times$ entropy, enthalpy, and free energy as a function of T ; (d) heat capacity versus T plot.

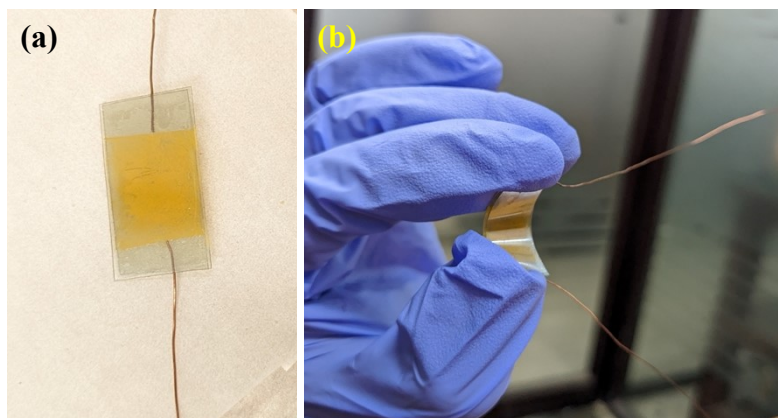


Figure S8: Picture of the PNG device (a) without bending (b) with bending.

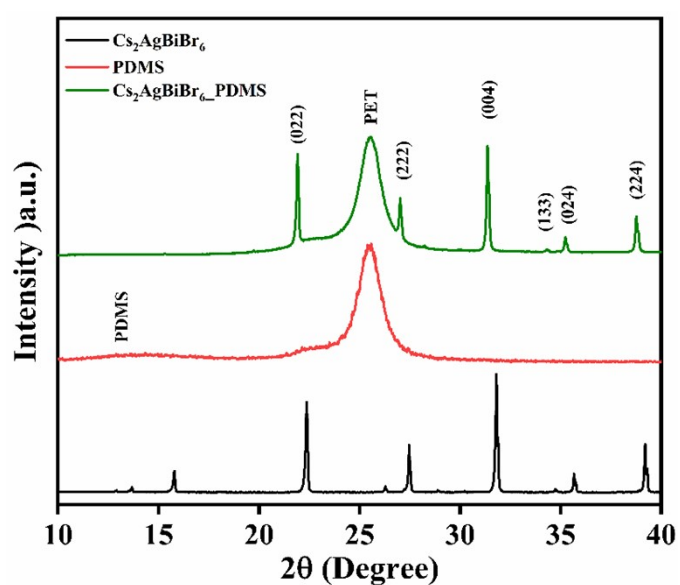


Figure S9: XRD of pure PDMS, $\text{Cs}_2\text{AgBiBr}_6$ crystals with prepared film

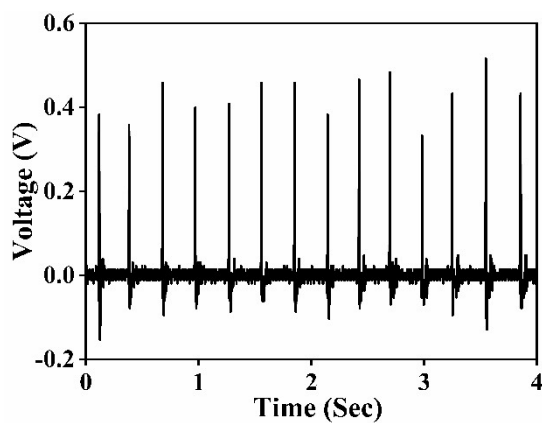


Figure S10: Output performance registered from PDMS

Group theoretical analysis using *VIBRATE!*

$\text{Cs}_2\text{AgBiBr}_6$

Hall Symbol: -F 4 2 3

Space Group: F m 3 m (O_h^5)

Space Group Number: 225

a = 11.2712

b = 11.2712

c = 11.2712

α = 90

β = 90

γ = 90

Crystal System: Cubic

Setting: Standard

Point Group: m3m (O_h)

Atomic Coordinates

24e	1	0.250310	0.000000	0.000000
24e	2	0.250310	0.500000	0.500000
24e	3	0.750310	0.000000	0.500000
24e	4	0.750310	0.500000	0.000000
24e	5	0.749690	0.000000	0.000000
24e	6	0.749690	0.500000	0.500000
24e	7	0.249690	0.000000	0.500000
24e	8	0.249690	0.500000	0.000000
24e	9	0.000000	0.250310	0.000000
24e	10	0.000000	0.750310	0.500000
24e	11	0.500000	0.250310	0.500000
24e	12	0.500000	0.750310	0.000000
24e	13	0.000000	0.749690	0.000000
24e	14	0.000000	0.249690	0.500000
24e	15	0.500000	0.749690	0.500000
24e	16	0.500000	0.249690	0.000000
24e	17	0.000000	0.000000	0.749690
24e	18	0.000000	0.500000	0.249690
24e	19	0.500000	0.000000	0.249690
24e	20	0.500000	0.500000	0.749690
24e	21	0.000000	0.000000	0.250310
24e	22	0.000000	0.500000	0.750310
24e	23	0.500000	0.000000	0.750310
24e	24	0.500000	0.500000	0.250310
4a	25	0.000000	0.000000	0.000000
4a	26	0.000000	0.500000	0.500000
4a	27	0.500000	0.000000	0.500000
4a	28	0.500000	0.500000	0.000000
4b	29	0.500000	0.000000	0.000000
4b	30	0.500000	0.500000	0.500000
4b	31	0.000000	0.000000	0.500000
4b	32	0.000000	0.500000	0.000000
8c	33	0.250000	0.250000	0.250000
8c	34	0.250000	0.750000	0.750000
8c	35	0.750000	0.250000	0.750000
8c	36	0.750000	0.750000	0.250000
8c	37	0.750000	0.750000	0.750000
8c	38	0.750000	0.250000	0.250000
8c	39	0.250000	0.750000	0.250000
8c	40	0.250000	0.250000	0.750000

Lattice Centring Operators

1: 0.000000 0.500000 0.500000

2: 0.500000 0.000000 0.500000

3: 0.500000 0.500000 0.000000

4: 0.000000 0.000000 0.000000

Non-Magnetic Case $k = 0$

Symmetry Operators

R	t	x,y,z	Operator: 1 (E)
1	0 0	0.000	
0	1 0	0.000	
0	0 1	0.000	

R	t	-y,-z,x	Operator: 3 (C₃)
0	-1 0	0.000	
0	0 -1	0.000	
1	0 0	0.000	

R	t	z,-x,-y	Operator: 3 (C₃)
0	0 1	0.000	
-1	0 0	0.000	
0	-1 0	0.000	

R	t	-y,z,-x	Operator: 3 (C₃)
0	-1 0	0.000	
0	0 1	0.000	
-1	0 0	0.000	

R	t	-z,-x,y	Operator: 3 (C₃)
0	0 -1	0.000	
-1	0 0	0.000	
0	1 0	0.000	

R	t	-z,x,-y	Operator: 3 (C₃)
0	0 -1	0.000	
1	0 0	0.000	
0	-1 0	0.000	

R	t	y,-z,-x	Operator: 3 (C₃)
0	1	0	0.000
0	0	-1	0.000
-1	0	0	0.000

R	t	z,x,y	Operator: 3 (C₃)
0	0	1	0.000
1	0	0	0.000
0	1	0	0.000

R	t	y,z,x	Operator: 3 (C₃)
0	1	0	0.000
0	0	1	0.000
1	0	0	0.000

R	t	-z,-y,-x	Operator: 2 (C₂)
0	0	-1	0.000
0	-1	0	0.000
-1	0	0	0.000

R	t	z,-y,x	Operator: 2 (C₂)
0	0	1	0.000
0	-1	0	0.000
1	0	0	0.000

R	t	-x,-z,-y	Operator: 2 (C₂)
-1	0	0	0.000
0	0	-1	0.000
0	-1	0	0.000

R	t	-x,z,y	Operator: 2 (C₂)
-1	0	0	0.000
0	0	1	0.000
0	1	0	0.000

R	t	-y,-x,-z	Operator: 2 (C₂)
0	-1	0	0.000
-1	0	0	0.000
0	0	-1	0.000

R	t	y,x,-z	Operator: 2 (C₂)
0	1	0	0.000
1	0	0	0.000
0	0	-1	0.000

R	t	-y,x,z	Operator: 4 (C₄)
0	-1	0	0.000
1	0	0	0.000

0 0 1 0.000

R	t	y,-x,z	Operator: 4 (C₄)
0 1 0	0.000		
-1 0 0	0.000		
0 0 1	0.000		

R	t	x,-z,y	Operator: 4 (C₄)
1 0 0	0.000		
0 0 -1	0.000		
0 1 0	0.000		

R	t	x,z,-y	Operator: 4 (C₄)
1 0 0	0.000		
0 0 1	0.000		
0 -1 0	0.000		

R	t	z,y,-x	Operator: 4 (C₄)
0 0 1	0.000		
0 1 0	0.000		
-1 0 0	0.000		

R	t	-z,y,x	Operator: 4 (C₄)
0 0 -1	0.000		
0 1 0	0.000		
1 0 0	0.000		

R	t	-x,-y,z	Operator: 2 (C₂)
-1 0 0	0.000		
0 -1 0	0.000		
0 0 1	0.000		

R	t	x,-y,-z	Operator: 2 (C₂)
1 0 0	0.000		
0 -1 0	0.000		
0 0 -1	0.000		

R	t	-x,y,-z	Operator: 2 (C₂)
-1 0 0	0.000		
0 1 0	0.000		
0 0 -1	0.000		

R	t	-x,-y,-z	Operator: 1 (i)
-1 0 0	0.000		
0 -1 0	0.000		
0 0 -1	0.000		

R	t	y,-x,-z	Operator: 4 (S₄)
0 1 0	0.000		

-1 0 0 0.000
0 0 -1 0.000

R **t** **-y,x,-z** **Operator: 4 (S₄)**
0 -1 0 0.000
1 0 0 0.000
0 0 -1 0.000

R **t** **-x,z,-y** **Operator: 4 (S₄)**
-1 0 0 0.000
0 0 1 0.000
0 -1 0 0.000

R **t** **-x,-z,y** **Operator: 4 (S₄)**
-1 0 0 0.000
0 0 -1 0.000
0 1 0 0.000

R **t** **-z,-y,x** **Operator: 4 (S₄)**
0 0 -1 0.000
0 -1 0 0.000
1 0 0 0.000

R **t** **z,-y,-x** **Operator: 4 (S₄)**
0 0 1 0.000
0 -1 0 0.000
-1 0 0 0.000

R **t** **-z,-x,-y** **Operator: 3 (S₆)**
0 0 -1 0.000
-1 0 0 0.000
0 -1 0 0.000

R **t** **-y,-z,-x** **Operator: 3 (S₆)**
0 -1 0 0.000
0 0 -1 0.000
-1 0 0 0.000

R **t** **y,z,-x** **Operator: 3 (S₆)**
0 1 0 0.000
0 0 1 0.000
-1 0 0 0.000

R **t** **-z,x,y** **Operator: 3 (S₆)**
0 0 -1 0.000
1 0 0 0.000
0 1 0 0.000

R **t** **y,-z,x** **Operator: 3 (S₆)**

0	1	0	0.000
0	0	-1	0.000
1	0	0	0.000

R	t	z,x,-y	Operator: 3 (S₆)
0	0	1	0.000
1	0	0	0.000
0	-1	0	0.000

R	t	-y,z,x	Operator: 3 (S₆)
0	-1	0	0.000
0	0	1	0.000
1	0	0	0.000

R	t	z,-x,y	Operator: 3 (S₆)
0	0	1	0.000
-1	0	0	0.000
0	1	0	0.000

R	t	x,y,-z	Operator: m (σ)
1	0	0	0.000
0	1	0	0.000
0	0	-1	0.000

R	t	-x,y,z	Operator: m (σ)
-1	0	0	0.000
0	1	0	0.000
0	0	1	0.000

R	t	x,-y,z	Operator: m (σ)
1	0	0	0.000
0	-1	0	0.000
0	0	1	0.000

R	t	z,y,x	Operator: m (σ)
0	0	1	0.000
0	1	0	0.000
1	0	0	0.000

R	t	-z,y,-x	Operator: m (σ)
0	0	-1	0.000
0	1	0	0.000
-1	0	0	0.000

R	t	x,z,y	Operator: m (σ)
1	0	0	0.000
0	0	1	0.000
0	1	0	0.000

$$\Gamma_{\text{red}} = A_{1g} + E_g + T_{1g} + 2T_{2g} + 5T_{1u} + T_{2u}$$

Irreducible representations (Bethe Notation)

$$\Gamma_{\text{red}} = \Gamma_1^+ + \Gamma_3^+ + \Gamma_4^+ + 2\Gamma_5^+ + 5\Gamma_4^- + \Gamma_5^-$$

Invariants

IR Active - Acoustic Modes (translations)

$$T_{1u} \quad \Gamma_4^- \quad (x, y, z)$$

Rotations

$$T_{1g} \quad \Gamma_4^+ \quad (R_x, R_y, R_z)$$

Raman Active

$$A_{1g} \quad \Gamma_1^+ \quad x^2 + y^2 + z^2$$

$$E_g \quad \Gamma_3^+ \quad (2z^2 - x^2 - y^2, x^2 - y^2)$$

$$T_{2g} \quad \Gamma_5^+ \quad (xz, yz, xy)$$

Silent

$$T_{2u} \quad \Gamma_5^-$$

References:

1. Pandey, R.; Gangadhar, S. B.; Grover, S.; Singh, S. K.; Kadam, A.; Ogale, S.; Waghmare, U. V.; Rao, V. R.; Kabra, D. Microscopic Origin of Piezoelectricity in Lead-Free Halide Perovskite: Application in Nanogenerator Design. *ACS Energy Letters* **2019**, *4*, 1004-1011.
2. Mallick, Z., Gupta, V., Jain, A., Bera, C. and Mandal, D., 2022. Utilizing Strain-Engineered Stable Halide Perovskite for Interfacial Interaction with Molecular Dipoles To Enhance Ferroelectric Switching and Piezoresponse in Polymer Composite Nanofibers. *Langmuir*, *39*(1), pp.320-333.
3. Zhang, Y., Parsonnet, E., Fernandez, A., Griffin, S.M., Huyan, H., Lin, C.K., Lei, T., Jin, J., Barnard, E.S., Raja, A. and Behera, P., 2022. Ferroelectricity in a semiconducting all-inorganic halide perovskite. *Science advances*, *8*(6), p.eabj5881.
4. Zhang, Q.; Solanki, A.; Parida, K.; Giovanni, D.; Li, M.; Jansen, T. L.; Pshenichnikov, M. S.; Sum, T. C. Tunable ferroelectricity in Ruddlesden–Popper halide perovskites. *ACS Appl. Mater. Interfaces* **2019**, *11*(14), 13523-13532.
5. Xiao, J.; Chang, J.; Li, B.; Isikgor, F. H.; Wang, D.; Fan, Z.; Lin, Z.; Ouyang, J.; Zeng, K.; Chen, J. Room temperature ferroelectricity of hybrid organic–inorganic perovskites with mixed iodine and bromine. *J. Mater. Chem. A* **2018**, *6*(20), 9665-9676.
6. Wang, Z. X.; Zhang, H.; Wang, F.; Cheng, H.; He, W. H.; Liu, Y. H.; Huang, X. Q.; Li, P. F. Superior transverse piezoelectricity in a halide perovskite molecular ferroelectric thin film. *J. Am. Chem. Soc.* **2020**, *142*(29), 12857-12864.
7. Zhang, H.Y., Song, X.J., Cheng, H., Zeng, Y.L., Zhang, Y., Li, P.F., Liao, W.Q. and Xiong, R.G., 2020. A three-dimensional lead halide perovskite-related ferroelectric. *Journal of the American Chemical Society*, *142*(10), pp.4604-4608.